UVA variability overrules UVB ozone depletion effects on the photoreduction of iron in the Southern Ocean

Rijkenberg, Micha J A; Gerringa, LJA; Neale, PJ; Timmermans, KR; Buma, Anita G J; de Baar, Hein J W

[Link to publication in University of Groningen/UMCG research database](#)

UVA variability overrules UVB ozone depletion effects on the photoreduction of iron in the Southern Ocean

Micha J. A. Rijkenberg,[1,2] Loes J. A. Gerringa,[3] Patrick J. Neale,[4] Klaas R. Timmermans,[3] Anita G. J. Buma,[1] and Hein J. W. de Baar[1,2]

[1] A spectral weighting function describing the wavelength dependency of the photoproduction of Fe(II) in Antarctic seawater was established. The strong wavelength-dependent photoproduction of Fe(II) from amorphous ferric hydroxides can be described as an exponential function: $\varepsilon(\lambda) = 3.57 \cdot 10^3 \cdot e^{-0.02(\lambda-300)}$. Solar spectra recorded during the 2000 Antarctic ozone depletion season were used to demonstrate that daily and seasonal variability of the ultraviolet A (UVA: 315–400 nm) and the visible part of the light spectrum (VIS: 400–700 nm) dominates Fe(II) production rates in surface waters (respectively >60% and about 30%) and in the water column. Although ultraviolet B (UVB: 280–315 nm) is the most effective wavelength region for Fe(II) photoproduction, the impact of UVB was small due to the relatively low flux of UVB into the ocean surface waters. However, the impact of UVB did indeed increase significantly from 3.54 to 6.15 % during the austral ozone minimum. *INDEX TERMS:* 4852 Oceanography: Biological and Chemical: Photochemistry; 1615 Global Change: Biogeochemical processes (4805); 1635 Global Change: Oceans (4203); 4207 Oceanography: General: Arctic and Antarctic oceanography; 4851 Oceanography: Biological and Chemical: Oxidation/reduction reactions. **Citation:** Rijkenberg, M. J. A., L. J. A. Gerringa, P. J. Neale, K. R. Timmermans, A. G. J. Buma, and H. J. W. de Baar (2004), UVA variability overrules UVB ozone depletion effects on the photoreduction of iron in the Southern Ocean, *Geophys. Res. Lett.*, *31*, L24310, doi:10.1029/2004GL020829.

1. Introduction

[2] The Southern Ocean plays an important role in controlling the CO_2 concentration in the atmosphere [*Hoppema et al.*, 1999]. Here biological fixation of CO_2 by phytoplankton in surface waters exceeds the expected outgassing of CO_2-rich upwelling waters [*de Baar and Boyd*, 2000]. However, extremely low iron (Fe) concentrations [*Martin et al.*, 1990] in concert with factors such as light and grazing [*de Baar and Boyd*, 2000] regulate primary production, species composition [*Buma et al.*, 1991] and carbon cycling within Southern Ocean planktonic communities. Various lines of evidence stress the great importance of the Fe(II) versus Fe(III) colloids oxidation/photoreduction cycle as the key process for keeping Fe available for uptake by plankton cells [*Johnson et al.*, 1994; *Wells et al.*, 1991].

[3] Effects of spectral changes on biological or chemical processes can be predicted by a spectral weighting function [*Neale et al.*, 1998a], a set of coefficients that, by multiplication with the energy of a discrete wavelength reveals its biological or chemical effect (here photoproduction of Fe(II)). Natural variations and anthropogenic perturbations of incoming solar irradiance (most importantly in the UV spectrum) play an important role in the plankton ecosystem of the Southern Ocean, as already shown using weighting functions for inhibition of photosynthesis [*Neale et al.*, 1998b] and DNA damage [*Karentz*, 1994].

[4] In this study we established a spectral weighting function for Fe(II) photoproduction in the Southern Ocean. This allows prediction of the impact on Fe(II) photoreduction of natural variability of irradiance, as well as the anthropogenic effect of increased levels of UVB due to springtime stratospheric ozone depletion. Freshly formed colloidal iron was the substrate, serving as the best possible simulation of colloidal iron formed upon an aeolian wet deposition dust event [*Hanson et al.*, 2001], after the supply of iron by melting sea-ice [*Sedwick and DiTullio*, 1997] or during an in situ Fe enrichment experiment [*Nishioka et al.*, 2005].

2. Experimental procedures

2.1. Experimental

[5] Southern Ocean surface seawater (44°S 20° E, 30th November 2000) (0.2 μm filtered) for the irradiation experiments was collected in an acid-cleaned tank (1 m^3) by means of an acid-washed braided PVS tubing attached to a torpedo towed alongside the ship (Polarstern, ANTXVIII/2). The tank was stored at room temperature for about a year.

[6] The 1 liter, UV transparent, polymethylmetacrylate (PMMA) bottles were pre-equilibrated with Southern Ocean seawater containing 10 nM Fe(III) (ammonium Fe(III) sulfate, Baker Analyzed, reagent grade). For each optical treatment a new PMMA bottle was prepared. The experiments were performed in a temperature controlled (4°C) class 100 clean container. The pH of the samples was 8.053 ± 0.051. The seawater was stirred with a Teflon stirring bean.

2.2. Fe in Southern Ocean Seawater

[7] Fresh colloidal iron was prepared by the addition of 10 nM Fe(III) to the seawater followed by overnight equilibration (12 hours, 4°C). Measurement of Fe, labile to 2-(2-Thiazolylazo)-p-cresol [*Croot and Johansson*,

---

[1]Department of Marine Biology, Centre for Ecological and Evolutionary Studies, University of Groningen, Haren, Netherlands.
[2]Also at Department of Marine Chemistry and Geology, Royal Netherlands Institute for Sea Research, Den Burg, Netherlands.
[3]Department of Marine Chemistry and Geology, Royal Netherlands Institute for Sea Research, Den Burg, Netherlands.
[4]Smithsonian Environmental Research Center, Edgewater, Maryland, USA.

2000], after a 50 nM Fe(III) addition showed that Fe colloid formation reached equilibrum within $2-3$ hours.

[8] The seawater contained 1.1 nM dissolved Fe and 1.75 ± 0.28 nM natural ligand with a conditional stability constant of $10^{21.75} \pm 10^{0.34}$. The excellent linear relationship between the initial Fe(II) photoproduction rate and the addition of three different concentrations Fe(III) in the range $10-20$ nM ($R^2 = 0.999$) showed that aging of Fe colloids did not play a substantial role in the Fe(II) photoproduction. The inability to destruct the Fe binding ligands with UV suggested that the natural ligands in the seawater were hardly photoreactive.

2.3. Light

[9] Philips UVB (TL-12), UVA (TL' 40W/05), VIS (TL'D 36W/33) lamps and 7 Schott optical cut-off filters (WG280, WG295, WG305, WG320, WG335, WG345 and WG360 nm) were used to create different optical treatments. Spectral conditions were measured for every treatment using a MACAM Spectroradiometer SR9910 with a spherical 4π sensor ($280-700$ nm). To prevent focussing effects during the experiments and measurement of the irradiance spectra (from inside a PMMA bottle) all sides of the box-shaped PMMA bottle, except the top, were covered with black plastic.

[10] PMMA bottles without a Schott filter received traces of wavelengths <280 nm (UVC). Using a spectrum ($270-400$ nm) of a Philips UVB (TL-12) lamp the spectra between 270 and 280 nm were reconstructed.

2.4. Weighting Function

[11] For each of the eight spectral treatments an exposure versus response curve was determined based on four different irradiance levels, each by measuring the concentration Fe(II) over time.

[12] The initial Fe(II) photoproduction rates (d[Fe(II)]/dt at t = 0, upon turning on the lights) were used to construct the weighting function. To establish the weighting function, weights were optimized to obtain the best fit with measured Fe(II) photoproduction using the equation:

$$\frac{\partial Fe(II)}{\partial t} = \sum \varepsilon(\lambda)E(\lambda)\Delta\lambda, \qquad (1)$$

where λ is the wavelength (nm), $\varepsilon(\lambda)$ is the weight (M m J^{-1}), i.e., effectiveness in photoproduction of Fe(II), at λ, and $E(\lambda)$ is the measured spectral irradiance (W m^{-2}) at λ.

[13] The spectral weighting function was determined by using iterative nonlinear regression (Marquardt method as implemented in the SAS NLIN procedure) to compute the best-fit parameters of an equation describing the wavelength dependence of $\varepsilon(\lambda)$ over the range 270 to 700 nm:

$$\varepsilon(\lambda) = W_{300} \cdot e^{-S_w(\lambda-300)}, \qquad (2)$$

where W_{300} is the weight at 300 nm (a reference wavelength) and S_w is the slope of the exponential function. The choice of a single slope exponential equation for the weighting function is general to a wide variety of chemical and biological effects [Neale and Kieber, 2000].

2.5. Iron(II) Analysis

[14] Concentrations of Fe(II) were followed using an automated flow injection analysis system employing a
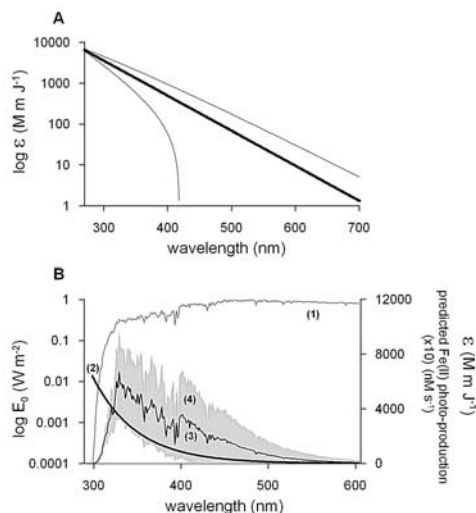

Figure 1. (a) The spectral weighting function (log ε scale) for the photoreduction of Fe in Southern Ocean seawater. The upper and lower lines represent the 95% confidence interval. (b) The solar spectrum (1) (log E scale (W m^{-2})), recorded on 22 Nov. 2000 (12:00 GMT) under ozone repleted conditions (370.4 DU), the weighting function (2) (ε (M m J^{-1})) and the resulting predicted Fe(II) photoproduction (3) (($\times$10) nM s^{-1}) with its 95% confidence interval (4) (light grey).

luminol-based chemiluminescence detection of Fe(II) [King et al., 1995]. An alkaline luminol solution (50 μM luminol in 0.5 M NH$_3$ (suprapur, Merck) and 0.1 M HCl (suprapur, Merck)) is mixed with the sample in a flow cell in front of a Hamamatsu HC135 photon counter. At pH 10, Fe(II) is rapidly oxidized by oxygen on a millisecond time scale causing the oxidation of luminol, producing blue light [Xiao et al., 2002]. Every 93 seconds a sample was transported in-line from the PMMA bottle into the flow cell using an 18.2 MΩ nanopure water carrier. The complete analysis system, reagents and tubing, were kept in the dark.

[15] Calibration was performed by standard addition to the sample matrix. The 0.01 M Fe(II) stock was prepared monthly by dissolving ferrous ammonium sulfate hexahydrate (Fe$^{(II)}$(NH$_4$SO$_4$)$_2$·6H$_2$O, Baker Analyzed, reagent grade) in 0.012 M 3xQD HCl. Working solutions were prepared daily. All Fe(II) stock solutions were refrigerated in the dark at 4°C if not in use.

[16] The time delay between Fe(II) addition and measurement caused oxidation. This oxidation was accounted for by extrapolating the data back to time zero because Fe(II) oxidation in seawater approximates pseudo-first-order kinetics.

2.6. Attenuation Coefficients, Solar Spectra and Ozone Concentration

[17] An attenuation spectrum determined in the Southern Ocean near Palmer station (data available at: www.lifesci. ucsb.edu/eemb/labs/prezelin/Public_datasets.html) [Boucher and Prezelin, 1996], the Beer-Lambert law and the weighting function were used to describe Fe redox cycling in the water column. Solar spectra and ozone concentrations for Palmer Station were recorded by respec-
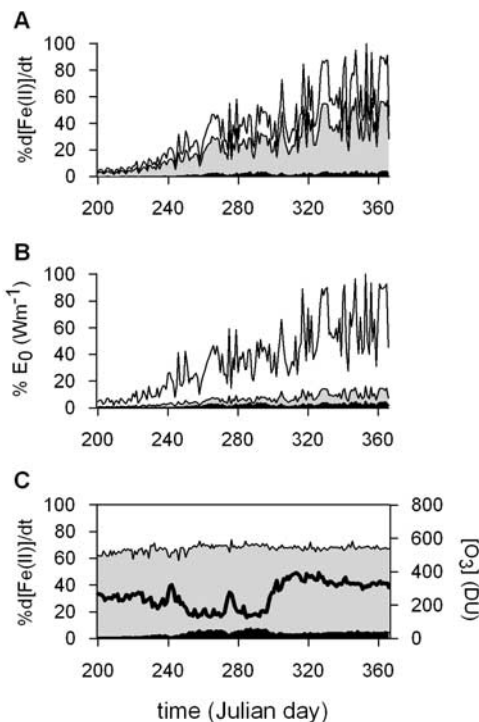
Figure 2. (a) Relative Fe(II) photoproduction rates in the surface ocean as a result of UVB (black), UVA (grey) and VIS (clear) exposure, using solar spectra from 18 July until 31 Dec. 2000 (16:00 GMT). Values were taken as percentage of the highest value for the Fe(II) photoproduction rate. (b) The relative intensities of incident UVB ($\times 10$) (black), UVA (grey) and VIS (clear) at the sea surface. Values were taken as percentage of the highest measured value for the light intensity. (c) The predicted relative Fe(II) photoproduction rate as a result of UVB (black), UVA (grey) and VIS (clear) and the concentration ozone in Dobson Units (DU) (black line). The Fe(II) photoproduction rates are relative to the Fe(II) photoproduction rate due to total irradiance each day.

tively the NSF Polar Programs UV Monitoring Network and the Total Ozone Mapping Spectrometer, NASA.

3. Results and Discussion

[18] The spectral weighting function for the photoproduction of Fe(II) from amorphous iron hydroxides showed the strongest Fe(II) production at the shortest wavelengths (UVB), the weight decreases about 2% for each nm increase in wavelength ($R^2 = 0.92$, $P < 0.0001$) (Figure 1a):

$$\varepsilon(\lambda) = 3.57 \cdot 10^3 \cdot e^{-0.02(\lambda-300)}, \tag{3}$$

[19] Upon application of the weighting function to a single solar spectrum collected in the morning (08.01 local time) under ozone repleted conditions near Palmer station, Antarctica (64.8°S, 64.1°W), the strong contribution of UVA (62%) to total solar radiation induced Fe(II) production was revealed (Figure 1b). Despite exhibiting very low weights, the visible part of the spectrum (VIS) was found to play a significant role (36%) (Figure 1b). The contribution

of UVB to Fe redox cycling was small (2.4%). The predicted maximum of the Fe(II) photoproduction rate occurred between 325 and 345 nm, at the shorter UVA wavelengths.

[20] When assessing the role of the three major wavelength bands on Fe(II) photoproduction throughout the major phytoplankton growth season (spring and summer), a large day-to-day variability was observed (Figure 2a). Yet on any given day, UVA was found to play the predominant role at a very steady 60%, followed by VIS at a quite uniform 35% (Figure 2c). In contrast, unweighted solar energy is primarily in the VIS band (83%) followed by UVA (16%) and UVB (0.3%) (Figure 2b). With the progression of the growth season the total Fe(II) photoproduction at midday doubled from early spring until early summer.

[21] Stratospheric ozone depletion in the austral spring results in significantly increased levels of UVB as well as spectral shifts in favor of the shorter UVB wavelengths. Under ozone depleted conditions the application of the weighting function continued to predict a major contribution of UVA of 63% of the total Fe(II) photoproduction rate followed by VIS, 31% (Figure 2c). Temporal decreases in ozone (between day 250 and 300; Figure 2c) coincided with an increase in UVB mediated Fe(II) photoproduction (>6%). After the ozone repletion (after appr. day 301) UVB related Fe photoproduction rates exceeded those in the preozone depleted period due to the higher solar zenith angle. This is further shown by application of the weighting function to two individual spectra recorded at Palmer station under ozone depleted and ozone repleted conditions respectively (Figure 3). Natural variations of the UVA and VIS effect on Fe photoreduction in surface waters, due to changing weather conditions, solar zenith angle etc., largely dwarf the significant (3.54% versus 6.15%) but
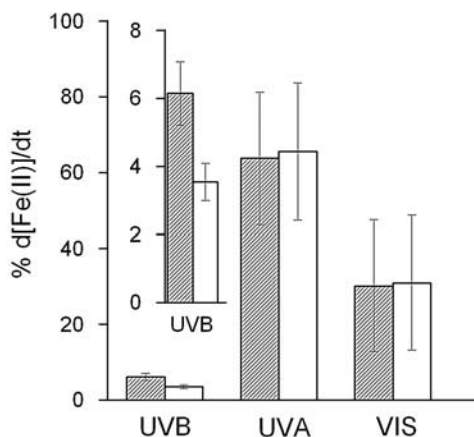

Figure 3. The wavelength band–dependent Fe(II) photoproduction as percentage of the photoproduction due to the total spectrum (280–605 nm) at 23 Sept. 2000 (16:00 GMT) (145.1 DU) and 9 Nov. 2000 (16:00 GMT) (389.9 DU). Incident UVB increased from 0.40% to 0.68% of solar irradiance. Insert: The difference in Fe(II) photoproduction rate due to UVB is significant (3.54% to 6.15%) and due to ozone depletion on 23 Sept. The uncertainty is given as the standard error derived from the weighting function.
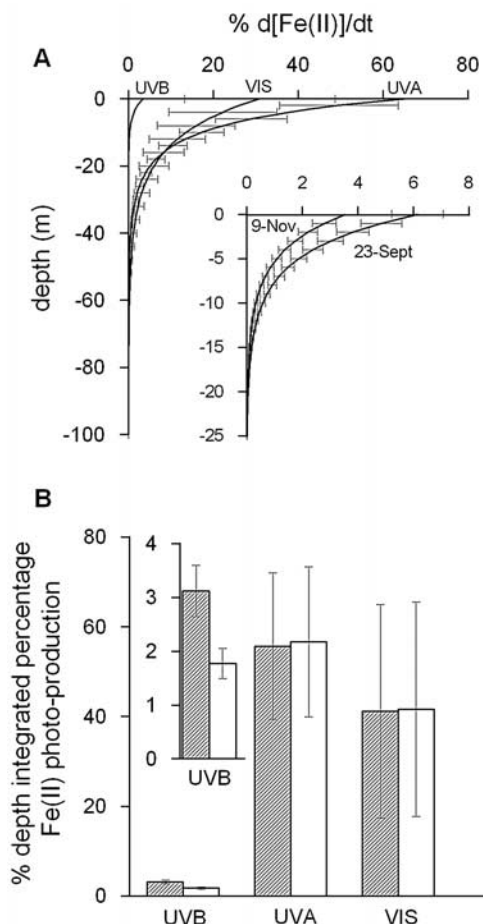
Figure 4. (a) The relative Fe(II) photoproduction rate due to natural UVB, UVA and VIS exposures (9 Nov. 2000, 16:00 GMT) with depth. Insert: The relative Fe(II) photo-production rate due to UVB at 23 Sept. 2000 (16:00 GMT) (145.1 DU) and at 9 Nov. 2000 (389.9 DU) with depth. Values are expressed as relative to the total irradiance at the surface. (b) The percentage depth integrated Fe(II) photo-production due to UVB, UVA and VIS for 23 Sept. (hatched) and 9 Nov. (non-hatched). Insert: The significant difference in depth integrated Fe(II) photoproduction due to enhanced UVB during ozone depletion. The uncertainties are given as standard errors derived from both the weighting function and the attenuation coefficients.

much smaller variations in UVB effect due to ozone depletion (Figure 3).

[22] Fe redox cycling as function of depth is shown in Figure 4a. Both natural and enhanced UVB were found to play a minor role in the upper 10 m water column for Fe(II) photoproduction (Figure 4a). Instead UVA and VIS were shown to be the most important wavelength regions within the water column. Because VIS penetrates deeper into the euphotic zone (1% Fe(II) photoproduction at 57 m depth) as compared to both UVB (1% Fe(II) photoproduction at 19 m depth) and UVA (1% Fe(II) photoproduction at 39 m depth), the VIS became more important with depth. Where Fe chemistry and bio-availability are affected by the Fe redox-cycle, UVA and VIS play an equally important role (Figure 4b) in contributing to depth integrated Fe(II) photoproduction.

[23] Sea ice causes strong attenuation of the solar spectrum, in the quantitative and the qualitative sense. As described UVB transmission through sea ice is highly variable [*Prezelin et al.*, 1998], fluctuating between <0.5% and 9% of incident UVB, as it depends on many characteristics such as ice thickness, snow cover, turbidity or brine inclusions. These characteristics also cause a large variability in UVB/UVA/PAR ratios. As a result, ice cover will have a large impact on Fe redox cycling in the water column below. When spectral attenuation characteristics of sea ice are known however, our spectral weighting function will allow for the determination of under ice Fe photoreduction.

[24] Our novel weighting function clearly shows that the UVA and the VIS govern the Fe photoreduction in Southern Ocean waters, in all seasons and at all depths. This function is now applicable in ecosystem models, in conjunction with suitable observed or modeled light spectra in open water and under the ice. Finally the natural day-to-day variability of UVA and VIS, completely overrides the enhanced UVB due to ozone depletion in the austral spring. Throughout the year, and even under ozone-depleted conditions, the role of UVB in the photo-induced redox cycle of iron is minor.

References

Boucher, N. P., and B. B. Prezelin (1996), Spectral modeling of UV inhibition of in situ Antarctic primary production using a field-derived biological weighting function, *Photochem. Photobiol.*, *64*, 407–418.

Buma, A. G. J., H. J. W. de Baar, R. F. Nolting, and A. J. van Bennekom (1991), Metal enrichment experiments in the Weddell-Scotia Seas—Effects of iron and manganese on various plankton communities, *Limnol. Oceanogr.*, *36*, 1865–1878.

Croot, P. L., and M. Johansson (2000), Determination of iron speciation by cathodic stripping voltammetry in seawater using the competing ligand 2–(2–thiazolylazo)-p-cresol (TAC), *Electroanalysis*, *12*, 565–576.

de Baar, H. J. W., and P. W. Boyd (2000), The role of iron in plankton ecology and carbon dioxide transfer of the global oceans, in *The Dynamic Ocean Carbon Cycle: A Midterm Synthesis of the Joint Global Ocean Flux Study*, edited by R. B. Hanson, H. W. Ducklow, and J. G. Field, Cambridge Univ. Press, New York.

Hanson, A. K., N. W. Tindale, and M. A. R. Abdel-Moati (2001), An equatorial Pacific rain event: Influence on the distribution of iron and hydrogen peroxide in surface waters, *Mar. Chem.*, *75*, 69–88.

Hoppema, M., E. Fahrbach, M. H. C. Stoll, and H. J. W. de Baar (1999), Annual uptake of atmospheric CO_2 by the Weddell Sea derived from a surface layer balance, including estimations of entrainment and new production, *J. Mar. Syst.*, *19*, 219–233.

Johnson, K. S., K. H. Coale, V. A. Elrod, and N. W. Tindale (1994), Iron photochemistry in seawater from the equatorial Pacific, *Mar. Chem.*, *46*, 319–334.

Karentz, D. (1994), Considerations for evaluating ultraviolet radiation-induced genetic-damage relative to Antarctic ozone depletion, *Environ. Health Perspec.*, *102*, 61–63.

King, D. W., H. A. Lounsbury, and F. J. Millero (1995), Rates and mechanism of Fe (II) oxidation at nanomolar total iron concentrations, *Environ. Sci. Technol.*, *29*, 818–824.

Martin, J. H., R. M. Gordon, and S. E. Fitzwater (1990), Iron in Antarctic Waters, *Nature*, *345*, 156–158.

Neale, P. J., and D. J. Kieber (2000), Assessing biological and chemical effects of UV in the marine environment: Spectral weighting functions, in *Causes and Environmental Implications of Increased UV-B Radiation*, edited by R. E. Hester and R. M. Harrison, pp. 61–83, R. Soc. of Chem., Cambridge, UK.

Neale, P. J., J. J. Cullen, and R. F. Davis (1998a), Inhibition of marine photosynthesis by ultraviolet radiation: Variable sensitivity of phyto-

plankton in the Weddell-Scotia Confluence during the austral spring, *Limnol. Oceanogr.*, *43*, 433–448.

Neale, P. J., R. F. Davis, and J. J. Cullen (1998b), Interactive effects of ozone depletion and vertical mixing on photosynthesis of Antarctic phytoplankton, *Nature*, *392*, 585–589.

Nishioka, J., S. Takeda, H. J. W. de Baar, P. Laan, P. Croot, M. Boye, and K. R. Timmermans (2005), Change in the concentrations of iron in different size fractions during an iron fertilization experiment in the Southern Ocean, EisenEx study, *Mar. Chem*, in press.

Prezelin, B. B., M. A. Moline, and H. A. Matlick (1998), *Icecolors 93: Spectral UV radiation effects on Antarctic frazil ice algae*, in *Antarctic Sea Ice: Biological Processes, Interactions and Variability, Antarct. Res. Ser.*, vol. 73, edited by M. P. Lizotte and K. R. Arrigo, pp. 45–83, AGU, Washington, D. C.

Sedwick, P. N., and G. R. DiTullio (1997), Regulation of algal blooms in Antarctic shelf waters by the release of iron from melting sea ice, *Geophys. Res. Lett.*, *24*, 2515–2518.

Wells, M. L., L. M. Mayer, O. F. X. Donard, M. M. D. Sierra, and S. G. Ackelson (1991), The photolysis of colloidal iron in the Oceans, *Nature*, *353*, 248–250.

Xiao, C. B., D. A. Palmer, D. J. Wesolowski, S. B. Lovitz, and D. W. King (2002), Carbon dioxide effects on luminol and 1, 10–phenanthroline chemiluminescence, *Anal. Chem.*, *74*, 2210–2216.

—————————

A. G. J. Buma, H. J. W. de Baar, and M. J. A. Rijkenberg, Department of Marine Biology, Centre for Ecological and Evolutionary Studies, University of Groningen, P.O. Box 14, NL-9750 AA Haren, Netherlands. (rijken@nioz.nl)

L. J. A. Gerringa and K. R. Timmermans, Department of Marine Chemistry and Geology, Royal Netherlands Institute for Sea Research, P.O. Box 59, NL-1790 AB Den Burg, Netherlands.

P. J. Neale, Smithsonian Environmental Research Center, P.O. Box 28, Edgewater, MD 21037-0028, USA.